NIST Special Publication 260
NIST SP 260-244

Certification of Standard Reference Material® 2246a

Relative Intensity Correction Standard for Raman Spectroscopy: 830 nm Excitation

Aaron A. Urbas
Kristine Gierz
Dennis D. Leber

NIST | NATIONAL INSTITUTE OF STANDARDS AND TECHNOLOGY
U.S. DEPARTMENT OF COMMERCE

This page intentionally blank.

NIST Special Publication 260
NIST SP 260-244

Certification of Standard Reference Material® 2246a

Relative Intensity Correction Standard for Raman Spectroscopy: 830 nm Excitation

Aaron A. Urbas
Chemical Sciences Division
Material Measurement Laboratory

Kristine Gierz
Dennis D. Leber
Statistical Engineering Division
Information Technology Laboratory

January 2024

Certain commercial equipment, instruments, software, or materials, commercial or non-commercial, are identified in this paper in order to specify the experimental procedure adequately. Such identification does not imply recommendation or endorsement of any product or service by NIST, nor does it imply that the materials or equipment identified are necessarily the best available for the purpose.

NIST Technical Series Policies
Copyright, Use, and Licensing Statements
NIST Technical Series Publication Identifier Syntax

Publication History
Approved by the NIST Editorial Review Board on 2024-01-16

NIST Author ORCID iDs
Urbas AA: 0000-0003-1535-5376
Gierz K: 0000-0002-4919-4841
Leber DD: 0000-0003-4179-5586

Contact Information
Please address technical questions you may have about this SRM to srms@nist.gov where they will be assigned to the appropriate Technical Project Leader responsible for support of this material. For sales and customer service inquiries, please contact srminfo@nist.gov

Abstract

Standard Reference Material® (SRM®) 2246a Relative Intensity Correction Standard for Raman Spectroscopy: 830 nm Excitation is intended for use in the correction of the relative intensity of Raman spectra obtained with Raman instruments employing 830 nm laser excitation. A unit of SRM 2246a consists of an optical glass that emits a broad-band luminescence spectrum when excited with 830 nm laser radiation. The shape of the mean luminescence spectrum of this glass is described by a mathematical expression that relates the relative spectral intensity to the wavenumber (cm^{-1}) expressed as the Raman shift from the 830 nm excitation laser wavelength. This model, together with a measurement of the luminescence spectrum of the standard, can be used to determine the spectral intensity response correction that is unique to each Raman system. The resulting instrument intensity response correction may then be used to obtain Raman spectra that are largely free from instrument-induced spectral artifacts. This publication documents the production, analytical methods, and computations involved in characterizing this product.

Keywords

Table of Contents

List of Tables

List of Figures

1. Introduction

Standard Reference Material® (SRM®) 2246a Relative Intensity Correction Standard for Raman Spectroscopy: 830 nm Excitation is a spectroscopic standard intended for use in the correction of the relative intensity of Raman spectra obtained with Raman instruments employing 830 nm laser excitation. SRM 2246a is the most recent member of the SRM 224x family of Raman intensity standards. The earlier members of this family are: SRM 2241 Relative Intensity Correction Standard for Raman Spectroscopy: 785 nm Excitation [1], SRMs 2242 and 2242a Relative Intensity Correction Standard for Raman Spectroscopy: 532 nm Excitation [2,3], SRM 2243 Relative Intensity Correction Standard for Raman Spectroscopy: 488 nm and 514.5 nm Excitation [4], SRM 2244 Relative Intensity Correction Standard for Raman Spectroscopy: 1064 nm Excitation [5], SRM 2245 Relative Intensity Correction Standard for Raman Spectroscopy: 632.8 nm Excitation [6], and SRM 2246 Relative Intensity Correction Standard for Raman Spectroscopy: 830 nm Excitation [7]. SRMs 2243 and 2245 have been discontinued.

SRM 2246a consists of an optical glass that emits a broad, featureless emission spectrum when excited with 830 nm laser radiation. The finished standard consists of a piece of optical glass secured in a microscope-style aluminum holder. For the correct use of this SRM, the standard is placed in the same position as an analytical sample whose measured spectrum is to be corrected for the instrument response.

The shape of the luminescence spectrum of this glass is modeled by a lognormal fit that relates the relative spectral intensity to the frequency expressed in Raman shift (units in cm^{-1} from 830 nm). The SRM is used to transfer a system-independent relative irradiance calibration to a given Raman spectroscopy system [8]. This facilitates the acquisition of Raman spectra that are instrument independent. This is important for the validation of the performance of Raman spectroscopy systems and the recording of spectra for inclusion in Raman libraries and spectral databases.

The relative spectral intensity of the SRM 2246a luminescence is calibrated based on careful comparisons to units of the previously certified SRM 2246. This is a departure from the previous process of calibrating the spectral response of multiple instruments with a NIST calibrated integrating sphere light source and deriving a certified model by consensus based on response corrected spectra from these instruments.

A separate stability assessment of SRM 2246 was conducted to both extend the certification period of SRM 2246 and provide additional confidence in the established model for use in certifying SRM 2246a.

1.1. Material and Processing

SRM 2246a is a chromium oxide doped (0.3 % mol fraction) borosilicate glass with the nominal composition as listed in Table 1.

Table 1. Nominal Composition of SRM 2246a Chromium-Doped Borosilicate Glass.

Component	Molar Mass g/mol	Mass g/100 g	Moles mol/100 g	Mole Fraction %
SiO_2	60.084	57.83	0.963	61.50
B_2O_3	69.618	21.79	0.313	20.0
Na_2O	61.979	14.56	0.234	15.0
Al_2O3	101.958	5.11	0.05	3.2
Cr_2O_3	151.990	0.714	0.005	0.3

Two melts of this glass were produced at NIST's Fabrication Technology Division. One of these melts was used to produce all units issued as the original SRM 2246. The remaining melt was used to produce SRM 2246a.

The component materials were melted and stirred in a platinum crucible in an open atmosphere furnace at 1360 °C. The molten glass was poured at 1380 °C and annealed at 560 °C for two hours. The annealing oven was then cooled from 560 °C to room temperature over 20 hours with a linear cooling rate averaging 27 °C/h.

The glass block was cut and finished by Starna Scientific Ltd (Ilford, UK) into nominally (10 × 10 × 1.65) mm units. The units are optically polished on one face and frosted to a 400-grit finish on the other.

1.2. Packaging

The SRM 2246a glass artifact is mounted in a microscope slide style optical holder designed to accommodate micro-Raman system optical measurement configurations. The artifact can be removed from this holder to accommodate other types of instrumentation. The holder dimensions are (25.4 × 76.2 × 3.00) mm ((1 × 3 × 0.118) in). In the center of the holder is a 1.63 mm (0.064 in.) deep rectangular slot approximately (10.2 × 26.4) mm ((0.4 × 1.05) in.) with an 8.00 mm (0.315 in.) diameter hole at its center. The glass artifact is retained in this holder by two Delrin springs. The holders are constructed of aluminum and anodized black after machining.

2. Spectrometer System

A single purpose-built Raman spectrometer system was used in the investigations and certification of SRM 2246a. The spectrometer system consisted of two optical measurement configurations, "micro-scale" and "macro-scale", based around a single emission path and spectrometer. The layout of this spectrometer system and some of the optical components were utilized in the certification of SRM 2242a. A schematic of the optical setup is shown in Fig. 1.
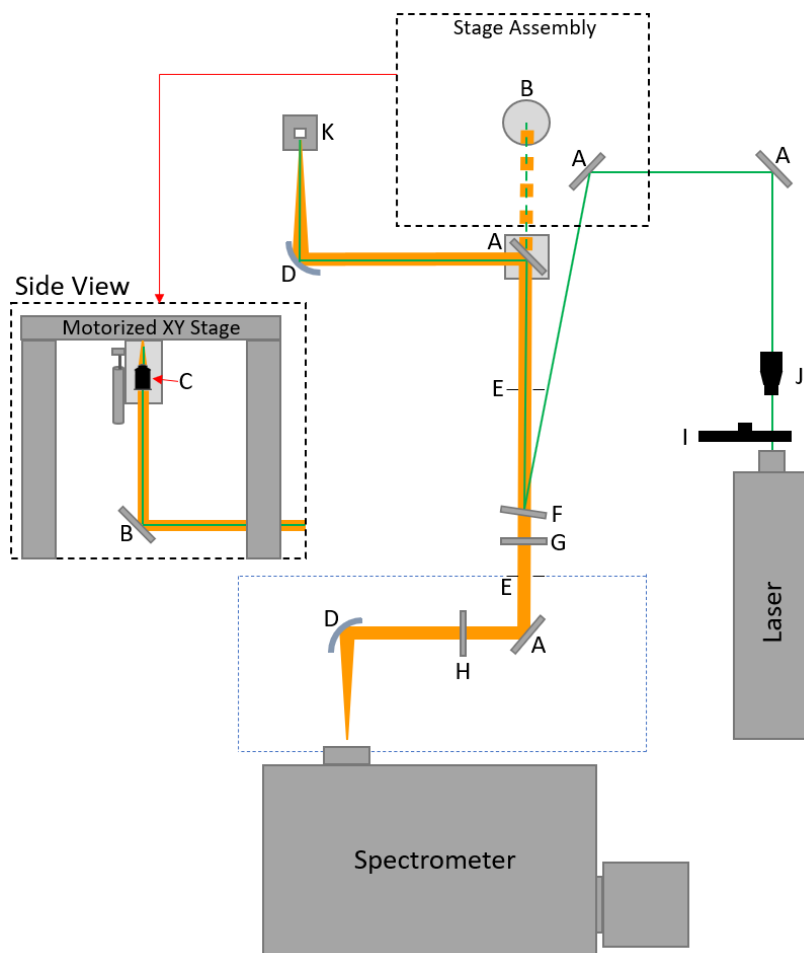
Fig. 1. Schematic of the optical setup of the Raman spectrometer system used.

A) 25.4 mm (1 in.) protected silver mirrors (Thorlabs, PF10-03-P01)
B) 50.8 mm (2 in.) protected silver mirror (Thorlabs, PF20-03-P01)
C) 4X microscope objective (Olympus PLAN S-APO 4X, "Super Apochromat")
D) 25.4 mm (1 in.) off-axis parabolic mirror with 101.6 mm (4 in.) reflected focal length (Thorlabs, MPD149-P01, protected silver coating)
E) Black anodized iris diaphragm with aperture adjusted to 12.7 mm (0.5 in.) diameter
F) 25 mm long-pass 830 nm filter (Semrock RazorEdge LP02-830RU-25, "U" grade, ≈120 cm^{-1} transition)
G) 25 mm long-pass 830 nm filter (Semrock RazorEdge LP02-830RE-25, "E" grade, ≈60 cm^{-1} transition)
H) 25.4 mm (1 in.) liquid crystal polymer microretarder depolarizer (Thorlabs, DPP25-B, AR Coating: 650 nm to 1050 nm)
I) Neutral density filter wheel for laser attenuation
J) Galilean 5X Beam Expander (ThorLabs, BE05)
K) temperature controlled cuvette holder (Quantum Northwest, Inc., model t2 Sport)

2.1. Configurations

The micro- and macro-scale configurations shared a common excitation laser source, a frequency stabilized 830 nm diode laser (Innovative Photonic Solutions, Monmouth, NJ model I0830SR0100B) with nominal open beam output power of 113 mW. Neutral density filters were used to attenuate the laser power as needed. The laser was allowed to warmup for at least 15 minutes prior to use. The laser wavelength was checked periodically with a Coherent WaveMaster laser wavelength meter (Coherent Inc, Santa Clara, CA) and consistently measured at 829.99 nm.

The two configurations shared a common optical path from the laser blocking filters to the spectrometer. The first laser blocking filter also served as a beam steering mirror to guide the laser onto the primary optical axis. For normal incidence this blocking filter has a specified nominal transmission edge of 120 cm^{-1} from 830 nm while the second blocking filter has a nominal transition edge 60 cm^{-1} from 830 nm. The angle of the first filter and the reflection angle of the laser was adjusted such that the transmission edge was slightly below that of second blocking filter for a beam trajectory along the primary optical axis. The efficiency of this filter for blocking the laser line along the primary axis was significantly reduced in this arrangement. However, this was remedied by utilizing the second blocking filter at normal incidence. The combination of the two filters passed very low levels of laser light relative to the SRM emission. Based on response corrected spectra, measurements of the emission spectrum of SRM 2246a were estimated to be minimally affected by filter transition effects above a Raman shift of approximately 70 cm^{-1} from 830 nm. The lower limit of the Raman shift range of the original certification of SRM 2246 was 110 cm^{-1} and the same limit was established for SRM 2246a. The Rayleigh scatter filtering performance in the optical system was, therefore, deemed suitable for the certification of SRM 2246a.

The micro- and macro-scale configurations were selectable by a removable mirror placed in the optical path and mounted on a kinematic stage to eliminate the need for realignment when switching. The "micro-scale" configuration was based on illumination and collection via a low magnification 4X microscope objective (Olympus PLAN S-APO 4X, "Super Apochromat") in a 180° backscatter (epiluminescence) geometry. A first surface mirror was used to steer the beam trajectory vertically with respect to the optical bench and into the back aperture of the objective lens. The objective was mounted on a motorized linear stage for vertical, Z-axis translation beneath a motorized XY stage (Aerotech Inc, Pittsburgh, PA, Model ALS36210-10) to provide illumination from below. The motorized linear stage was used to adjust the focal point of the microscope objective relative to samples placed on the XY stage. The XY stage can accommodate replaceable inserts for various sample formats and a custom anodized aluminum insert for the stage was fabricated by the NIST Fabrication Technology Division to hold 36 SRM units (10 mm × 10 mm), in a 6 × 6 grid pattern. This insert was used for automated mapping purposes for homogeneity assessment and certification measurements.

The macro-scale measurement configuration was based on illumination and collection using a 25.4 mm (1 in.) off-axis parabolic mirror with a 101.6 mm (4 in.) reflected focal length. This was used to provide illumination/collection setup with minimal spherical or chromatic aberrations. A temperature-controlled cuvette holder was typically used in this setup for sample introduction. The cuvette holder was mounted on a linear translation stage to allow for sample positioning along the beam path.

A 30 mm cage filter cube assembly was used for white light and pen lamp calibrations in this macro-scale configuration. This cage assembly was post mounted and required removal of the cuvette holder from the sample position for use. An iris aperture was placed between the white light calibration source and the assembly to restrict illumination largely to the internally mounted sintered polytetrafluoroethylene (PTFE) diffuse reflector. Certification measurements, SRM 2246 stability measurements, and additional temperature studies of SRM 2246a were conducted using this configuration.

The spectrograph was a 320 mm focal length, f/4.6, aberration corrected IsoPlane SCT-320 imaging spectrograph (Princeton Instruments, Acton, MA) equipped with a PIXIS 400BR eXcelon (Princeton Instruments) back-illuminated, deep-depletion, TE cooled (-70° C), 1340 pixel × 400 pixel (20 µm pixels) charge-coupled device (CCD) detector. The spectrometer was controlled by the LightField software (Princeton Instruments). LightField integration with LabView was utilized to synchronize data acquisition with the XY stage.

2.2. System Spectral Response Calibration (Y-Axis)

White light and pen lamp calibrations were performed using the 30 mm cage filter cube assembly with internally mounted sintered PTFE disk. White light calibrations were only performed on the all-reflective macro-scale configuration that utilized the off-axis parabolic mirror. The results of the white light calibrations were used for comparison purposes of the corrected SRM 2246 spectra with the SRM 2246 certified lognormal model and not for certification of the corrected emission spectrum of SRM 2246a. These comparisons were consistent with the confirmation of the stability of SRM 2246 that had previously established during a stability assessment of SRM 2246 conducted in 2022.

The certified model for SRM 2246a was based on corrected spectra generated from response calibrations utilizing SRM 2246. Multiple units were measured under identical conditions and at the same time as SRM 2246a units. Since the glass artifacts are the same dimensions and are finished the same (frosted on one face, polished on the other) these measurements were relatively straightforward. Individual spectral intensity correction curves were generated at each grating position. The spectral intensity correction curve is obtained by dividing the calibration curve data of the reference by the measured spectrum of the reference. For white light calibration sources in the past, the calibration data was derived from the calibrated irradiance data provided on the calibration report. For SRM 2246, the calibration curve is the certified linearly shifted lognormal model. Corrected Raman or SRM luminescence spectra are then obtained by multiplying by the spectral intensity correction curve. For multiple grating positions, spectra corresponding to each grating position were intensity-corrected separately and normalized by the area in the overlapping regions to correct for small discontinuities in intensity between the two spectra.

All SRM data was recorded in wavelength (nm) units. Dark spectra were subtracted with the SRM removed but with the laser left on. SRM spectra were converted into absolute wavenumber units using an appropriate radiometric conversion and finally to Raman shift relative to the excitation laser line position. For most investigations the corrected SRM spectra were normalized by dividing by the area under the curve corresponding to the certification range of (110 to 3000) cm^{-1} Raman shift. After normalization an additional scaling factor was applied across the model certification data set such that the maximum value of the certified model was equal to unity. For comparisons of other data sets (e.g., homogeneity and temperature

dependence) to the model additional scaling factors after area normalization were similarly used such that the average spectrum of the data set had a maximum value of 1 to correspond with the model.

The SRM 2246a certified model, $I_{SRM}(\Delta\upsilon)$, is a unitless photon flux ratio expressed as (photons per wavenumber)/(spectral maximum photons per wavenumber). The relative luminescence spectrum is traceable to the NIST spectral radiance scale [9] through comparison measurements to SRM 2246. The relative luminescence spectrum of SRM 2246 was calibrated using a white light, uniform, integrating sphere source that had been calibrated for irradiance at NIST and a high emissivity black body radiator with furnace temperature calibrated by the manufacturer. The calibration units of the irradiance of the white light source are Watt/(cm^2 nm) or an equivalent thereof. These units are converted to a photon flux per wavenumber for use in Raman spectrometers that typically utilize CCD detectors, which are photon-counting devices. The wavenumber unit (cm^{-1}) is the reciprocal of the wavelength expressed in centimeters. The unit Watt is converted to the number of photons n from the Planck relation $n = E\lambda/hc$, where E is the energy in watts, λ is the wavelength in nm, h is Planck's constant (J s), and c is the speed of light (m s^{-1}). Conversion from the wavelength scale to the wavenumber scale requires an additional multiplication by a factor of λ^2 since the physical expression for the measured irradiance is an integral equation, $-\delta\upsilon = 1/\lambda^2\ \delta\lambda$. [10]

2.3.   System X-Axis Calibration

The absolute X-axis calibrations of the spectrometer systems were conducted using emission lines from a Ne pen lamps[11,12]. Pen lamp data was recorded in wavelength (nm) units and X-axis calibration was performed in wavelength (nm). For the certification of the emission spectrum over the full spectral range, two overlapping grating positions were used. For some investigations (e.g., homogeneity assessment) single grating positions were used. The accuracy of the pen lamp line positions after offline calibration were within ± 0.05 nm, which corresponds to a wavenumber accuracy of approximately ± 0.7 cm^{-1} or better (less) across the relevant spectral range. Wavelength calibrations or checks were performed periodically and when switching between configurations or performing realignment of optical components. Periodic wavelength calibration checks showed that the wavelength calibrations were stable within ± 0.1 nm over time (weeks) and when repositioning the grating.

The laser wavelength was verified as describe above using a Coherent WaveMaster laser wavelength meter. When resolution permitted, the measured locations of Raman bands of cyclohexane and benzonitrile were used to check the final Raman shift calibration by comparison to the established Raman shift positions of the bands in the ASTM Raman shift guide [13]. The overall day-to-day intermediate precision of the Raman shift axis was estimated to be ± 2 cm^{-1} or less, which was deemed suitable for this certification.

2.4.   Spectral Processing

All spectral processing was performed in Matlab 2022a and 2023a (Mathworks Inc. Natick, MA).

3. Characterization Studies

3.1. Homogeneity Assessment

For SRM 2246a, a full batch homogeneity assessment was conducted using established procedures. The homogeneity data for the full lot of SRM 2246a units was collected over eight days. In brief, 158 SRM 2246a units were initially evaluated by visual inspection in ambient laboratory lighting and on a polariscope to look for evidence of striae or strain in the glass. Following this, a homogeneity assessment was conducted based on emission spectra collected from a 32×32 grid scan (1024 locations in total) covering a square area of (7×7) mm around the center of each unit of the SRM surface. This corresponds to steps of approximately 220 μm in each dimension between scanning locations. The screening data for these units was also utilized in the determination of the overall homogeneity of the batch certified material.

To compensate for instrumental drift or lab temperature fluctuations that could occur during the homogeneity assessment, a single SRM 2246a unit was scanned (across 49 locations) as a reference between every 2246a test unit. The same 2246a reference unit was used during the entire homogeneity assessment. Data from the reference unit collected immediately before and after a specific SRM 2246a unit being tested was used to perform a relative intensity correction of the test unit data using a preliminary fit of the lognormal model. This corrected data was used solely for the purposes of assessing homogeneity across the batch and not for model certification purposes, so the accuracy of the intensity correction for this stage was not critical. At the conclusion of the full batch screening process, described in more detail below, 113 units were retained for sale.

3.2. Temperature Dependence

SRM 2246a is certified for use between 20 °C and 25 °C. SRMs in the 224x series generally exhibit temperature dependencies. Within this temperature range, the effects are not large but readily measurable. A temperature study was conducted on SRM 2246a over this range using the temperature-controlled cuvette holder (Quantum Northwest, Inc., model t2 Sport). Three SRM 2246a units were encased in a custom 1 cm cuvette-sized anodized aluminum block (fabricated by the NIST machine shop) placed in the temperature-controlled cuvette holder for this study. Data was collected at 20.0 °C, 22.5 °C and 25.0 °C at a single grating position that covered the Raman shift range from approximately 68 cm^{-1} to 2882 cm^{-1}. The temperature was allowed to stabilize for at least 5 minutes after changing temperature or replacing samples. Test spectra were collected prior to the study to verify that this was enough time to reach equilibrium. Ten repeat spectra were collected for each measurement. The collected data at all temperatures was normalized in the same manner as described above (area under the curve), noting that the spectral range covered by this data set only extended to a Raman shift of 2882 cm^{-1}.

3.3. Laser Power Dependence

Following the release of SRM 2246, a presumed heating effect with increasing laser powers was discovered that impacts the use of the SRM. It was subsequently determined that the laser power levels used for most of the certification measurements of SRM 2246 would have resulted in relatively negligible heating effects. Stability studies were conducted at much higher laser

powers but the purpose of these was to ascertain whether any degradation of the glass resulted from exposure to higher laser power levels. For SRM 2246a, investigations were conducted on both micro- and macro-scale measurement configurations of the spectrometer system to look at perturbations of the emission peak profile with varying laser power levels to provide guidance to users of the SRM.

3.4.   Certification of Relative Emission Model

Three data sets were used to establish the certified model for the corrected emission spectrum of SRM 2246a. Two sets were collected on the macro-scale configuration over three days at 22.5 °C using the temperature-controlled cuvette holder. One set was collected on the micro-scale configuration at ambient laboratory temperature, typically (22 to 23) °C. No special controls were made for humidity other than the building air handling system, nominally (30 to 50) %.

The data consisted of spectra collected at two overlapping grating positions and covered a Raman shift range, relative to 830 nm, of at least 110 cm^{-1} to 3000 cm^{-1}, which are the limits of the certification range. The lognormal model was fit to the full range of the available data, from approximately 60 cm^{-1} to 3600 cm^{-1}. The high wavenumber limit of this range, 3600 cm^{-1}, corresponds to approximately 1184 nm. While a back-illuminated infrared-enhanced CCD was used here, the quantum efficiency falls off sharply approaching and beyond 1100 nm. The resulting corrected spectra exhibited rapidly diminishing signal-to-noise towards the high Raman shift end of the spectrum, but the data was deemed suitable for use in fitting over the extended range. A corrected SRM 2246a extended spectrum and a lognormal fit is shown in Fig. 2.
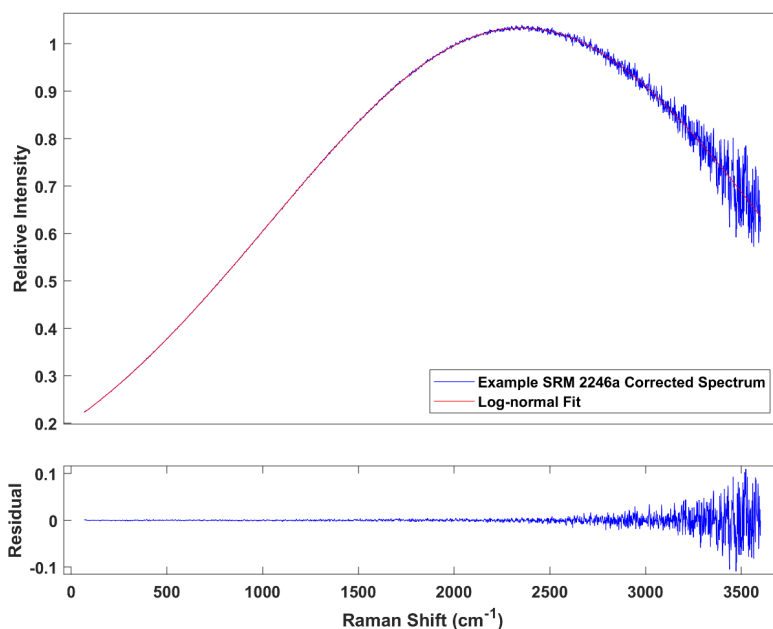

Fig. 2. Example of a Corrected SRM 2246a Spectrum.

Top Panel: SRM 2246a spectrum corrected for the relative response using SRM 2246 and a lognormal fit to the data. Bottom Panel: Residuals from the lognormal fit to the corrected spectrum. This spectrum was spliced together from two overlapping spectra for presentation purposes.

Based on experience, corrected SRM spectra using calibrated light sources with similar types of CCD detectors often exhibit artifacts or other anomalies this far into the near infrared. In the present work, the corrected SRM 2246a spectra were expected and found to be largely free of these types of issues because the response correction was derived from a nearly identical emission spectrum (SRM 2246 units) generated from the same artifact geometry (glass thickness and surface finish).

Spectra from the overlapping grating positions were normalized to the area under the overlapping region after response correction to ensure continuity in the emission profile between the spectra. The differences in intensity in the overlap regions prior to this normalization were typically small and may be attributable to slight laser power fluctuations between acquisitions.

For the purposes of fitting the lognormal model, spectra were intensity normalized but not spliced together into a single continuous spectrum. As with SRM 2246, an evaluation of the lognormal model indicated that the data could be fit to the extended range without negatively impacting the goodness of fit in the certification range. To give a peak maximum of approximately one in the resulting certified lognormal model, a universal scaling constant was determined from a preliminary fit and applied to all curves.

4. Results

4.1. Homogeneity Assessment

The spectral data from the homogeneity screening of each of the 158 units was evaluated by examining several plots. Two replicate spectra were collected from each of the 1024 (32 × 32 grid) locations sampled. Comparison of the replicate spectra pairs was used to automatically filter out cosmic ray spikes in individual spectra. Data in spectral regions corresponding to identified spikes (typically narrow regions consisting of only a few pixels) was replaced by linearly interpolation. This approach is effective in this case due to the broad, featureless, profile of the SRM emission spectrum but may not (or likely would not) be suitable for Raman spectra containing sharp peaks. After spike filtering, the spectral data for each unit were intensity corrected using a preliminary lognormal 2246a model using the average spectrum from the reference 2246a unit scanned before and after each test unit. This relative intensity correction was only used for the purposes of removing small pixel to pixel sensitivity variations (fixed pattern noise) as well as minor ripple artifacts observed in the spectra attributed to a combination of filter and CCD etaloning.

After relative intensity correction, the only remaining significant source of variance that hindered assessing peak shape homogeneity was a random noise component in all spectra, largely attributable to Poisson distributed shot noise. To eliminate this, a 5th order polynomial was fit to each spectrum in the relative intensity corrected data set. It was unknown whether this polynomial model would be too rigid to capture significant shape deviations in the emission profile in individual spectra compared to the overall average. To check the effectiveness of the fit, individual spectra with the largest residuals, gauged by the residual sum of squares, were examined to look for evidence of non-random structure but no issues were observed. After fitting the 5th order polynomials, each spectrum was normalized by the total area under the curve.

From the homogeneity assessment of each unit, a set of four plots were generated to evaluate whether to retain or reject the unit for release. An example of the plots is provided in Fig. 3.
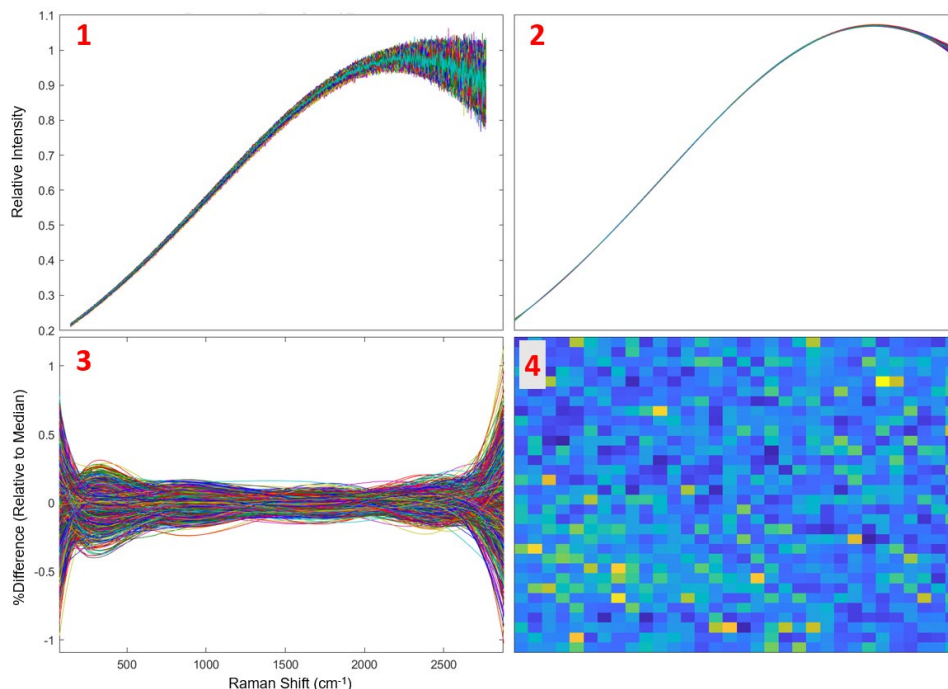

Fig. 3. Example of Ideal Homogeneity Screening Data Set.

Panel 1) The spike-filtered, relative intensity corrected data set.
Panel 2) The polynomial-fitted, area normalized data set.
Panel 3) The difference of each spectrum relative to the median of the data set, expressed as a percentage.
Panel 4) The summed absolute values of the Panel 3 data plotted as an image based on the spatial locations scanned.

Panels 3 and 4 are the most diagnostic in determining whether to reject units. The "heat map" of Panel 4 is used to look for spatial patterns in the glass that correlate with variability in the emission profile. The map's color scale is determined for each unit. In Panel 3, the difference spectra should generally lie within an interval of ±1 % relative to the data set median. Some deviations at the edges of the spectra are acceptable and are a consequence of the polynomial fitting. One or two anomalous spectra were permitted as long as they were not very near the center of the unit or represented a very significant outlier (e.g., outside a ±5 % interval).

The heat map is inspected to look for clear signs of spatial inhomogeneity in the emission profile. These are assumed to be from striae or inclusions in the glass matrix. Due to the unit-dependent scaling of the color scale in this panel it is quite sensitive at revealing subtle spatial homogeneity issues even when the spectral data for the unit as whole exhibits relatively low variance. Consequently, any heterogeneity or patterns observed in Panel 4 should be considered relative to the spectral data in Panel 3.

This evaluation process involves some subjective judgment by the analyst. The data from the SRM 2246a unit depicted in Fig. 3 represents a relatively ideal unit. Results for wo units that were accepted despite anomalies are depicted in Fig. 4 and Fig. 5. Results for two units that were not accepted are depicted in Fig. 6 and Fig. 7.
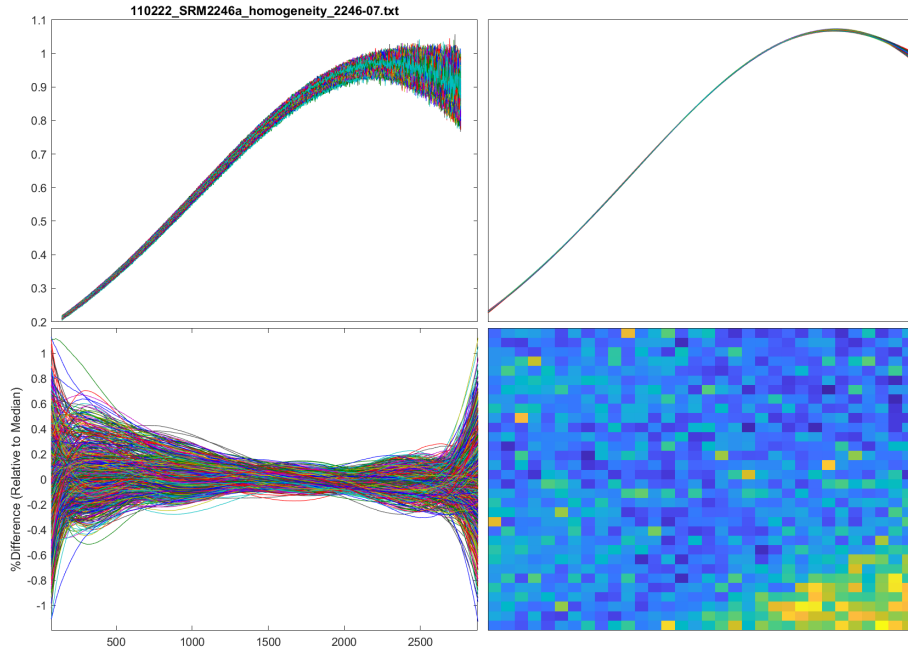
Fig. 4. Example of a Unit with Acceptable Spatial Heterogeneity.

The spectra in the bottom left panel were still well within the ± 1 % interval.
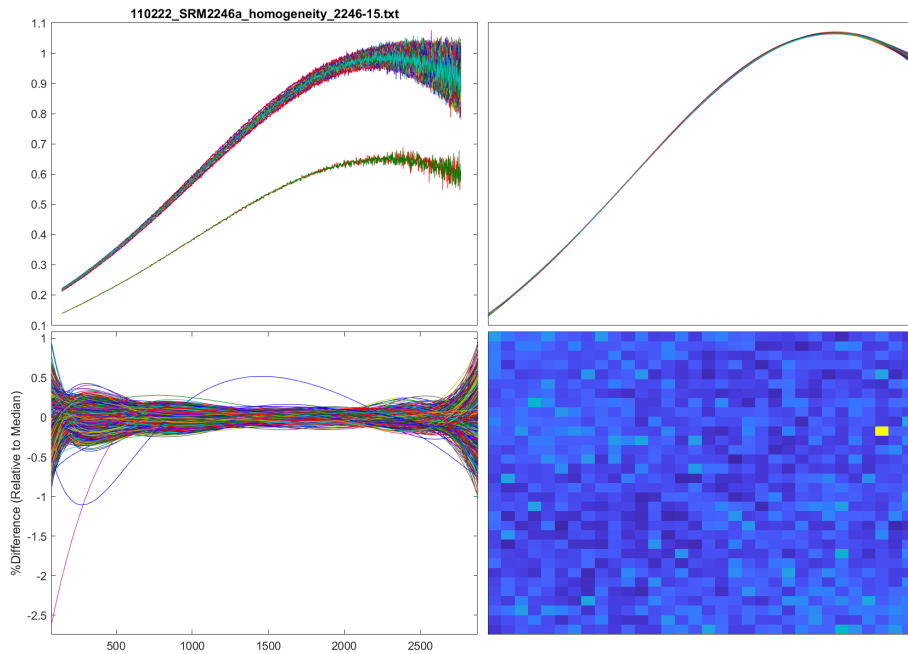
Fig. 5. Example of a Unit with an Acceptable Number of Anomalous Spectra.

The small number of anomalous emission spectra are away from the center of the unit.
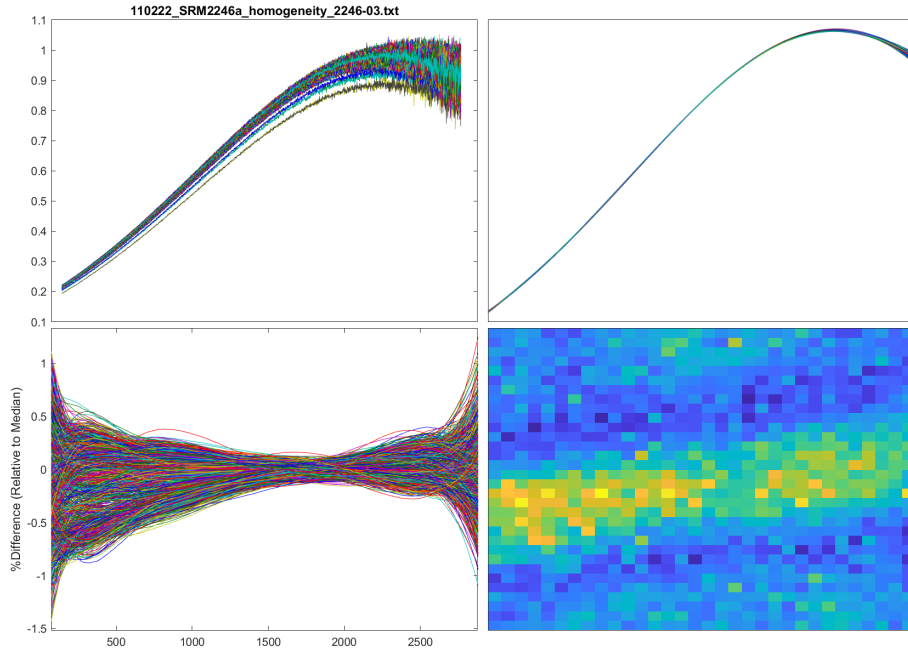
Fig. 6. Example of a Unit with Unacceptable Spatial Heterogeneity.

The spectra in the bottom left panel are still largely within the ± 1 % interval but the unit was not passed due to the striping seen in the bottom right panel through the center of the unit.
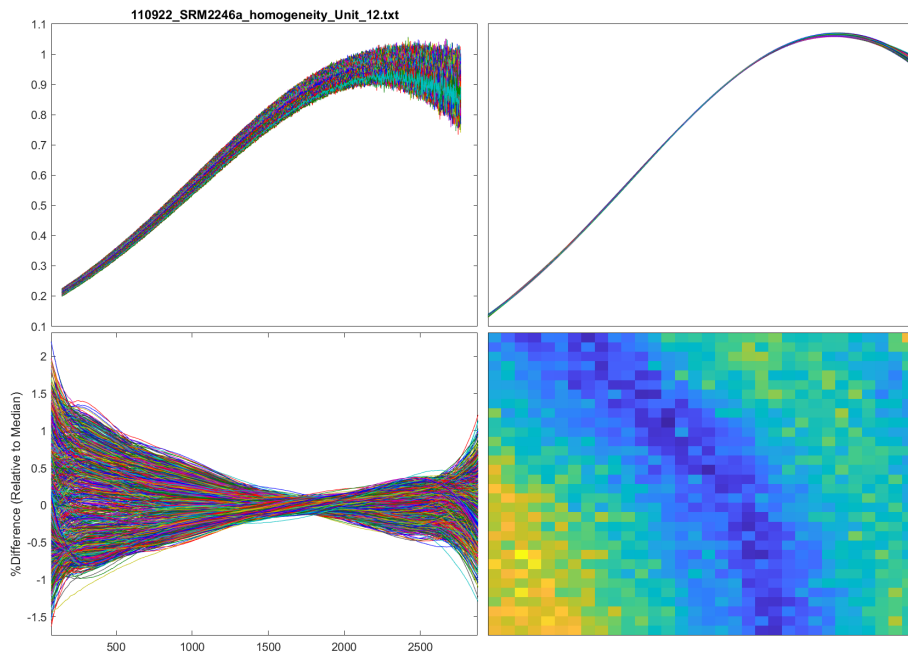
Fig. 7. Example of a Unit with Unacceptable Deviations and Spatial Heterogeneity.

A large number of spectra in the bottom left panel start to deviate from the ± 1 % interval in the low wavenumber range and striping is observed in the bottom right panel throughout the unit.

This visual examination and grid sampling approach should lead to the discovery of larger scale imperfections in the glass units but does not eliminate the possibility that smaller localized irregularities may be present in units that passed inspection.

After inspection and homogeneity screening of the full lot of units, 113 were retained for release as SRM 2246a. The overall homogeneity of the release units was assessed by calculating average spectra for each unit using the homogeneity data. These spectra were normalized by the area under the curve and then an additional scaling factor applied such that the maximum of the grand mean spectrum over all units was one. This spectrum is shown in Fig. 8, along with the percent relative standard deviation of the spectra for the acceptable units. This data set was used in the estimation of a homogeneity related uncertainty component.
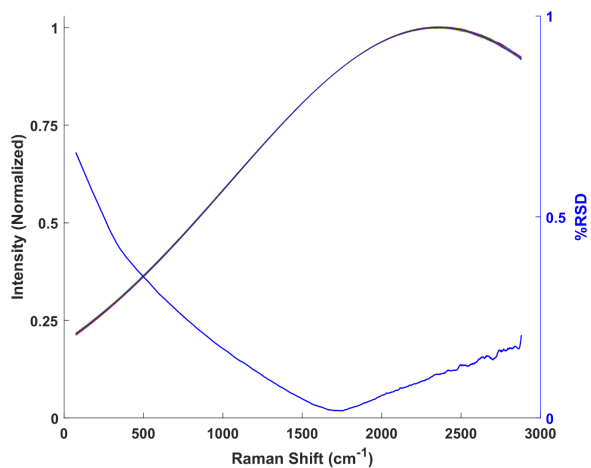
Fig. 8. Grand Mean Intensity and Relative Standard Deviation.

The upper smooth curves represent the overlaid area-normalized average emission spectra of the 113 accepted SRM 2246a units. The lower somewhat irregular curve represents the relative standard deviation of these spectra, expressed as a percentage of the mean intensity.

4.2. Temperature Dependence

Three SRM 2246a units were measured in the temperature study at (20.0, 22.5, and 25.0) ºC. The average spectrum of one of these units at the three temperatures (without intensity normalization) is shown in Fig. 9. The average spectrum of the 3 units at 22.5 ºC was used to generate a relative response correction based on a preliminary lognormal model of SRM 2246a. The response correction was then used to correct all collected spectra for this study.
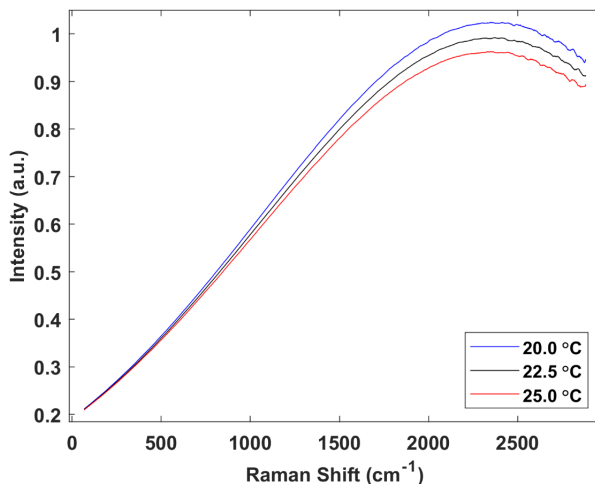
Fig. 9. Average Spectra Measured at (20.0, 22.5, and 25.0) ºC.

The absolute emission intensity decreases with increasing temperature. A less evident trend is a slight blue shift (towards the laser line) in the emission peak with increasing temperature. This is more readily visualized in Fig. 10 where the spectra have been normalized by the total area under the curve and plotted as differences relative to the mean of the three 22.5 ºC spectra.
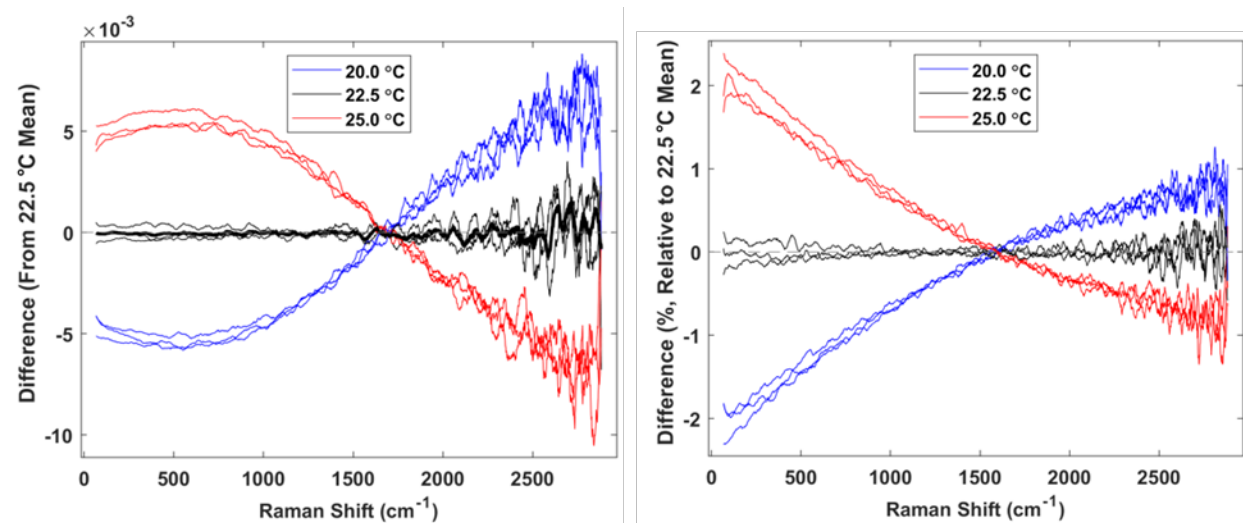
Fig. 10. Spectral Shift as a Function of Temperature.

Left panel: The difference spectra relative to measurements conducted at 22.5 °C.
Right panel: The same data set plotted as a percent relative to the mean spectrum at 22.5 °C.

The magnitude of the peak shifts with temperature are consistent between the units. The SRM is certified for use between 20 ºC and 25.0 ºC and this data set was used to estimate a temperature related component of uncertainty. The laser power used in the temperature study was kept below the threshold where laser induced temperature effects, described in the following section, were observed.

4.3. Laser Power Dependence

Investigations were conducted on both the micro- and macro-scale measurement configurations to look for perturbations of the emission peak profile with varying laser powers. The spot size at the focal point of the macro-scale configuration was estimated at 250 µm using a scanning knife edge beam profiler (ThorLabs WM100 Omega Meter). Laser power was measured at the sample position and controlled by a series of neutral density filters. SRM 2246a units were illuminated at the lowest laser power (≈0.3 mW) at the outset. Prior to data collection, units were allowed to equilibrate for 5 minutes initially and then after each power increment. Changes in emission profile were investigated by normalizing spectra by the total area under the curve and then examining differences relative to the spectrum at the lowest laser power. The laser heating effect was consistent across the three units. The differences observed for a single unit and for the mean of the three units are displayed in Fig. 11.

Fig. 11. Spectral Shifts as a Function of Laser Power in the Macro-Scale configuration.

Left panel: Difference spectra of one SRM 2246a unit when excited at different laser powers relative to measurements conducted at the lowest laser power. The lines for the highest power represent repeated measurements over a two h interval. The dotted blue and red lines around zero difference represent measurements at 0.3 mW and 1.7 mW, respectively, conducted after measurements taken at higher powers in the same location.

Right panel: Average difference spectra for three SRM 2246a units when excited at different laser powers relative to measurements conducted at the lowest laser power.

While relatively minor, perturbations to the peak profile are already evident at 5.9 mW and become progressively more substantial as the laser power increases. After reaching equilibrium the spectrum is quite stable over time. When the laser power is reduced back to lower powers, the original emission profile is restored. This procedure was repeated with three SRM 2246a units and the relative peak shifts at different laser powers were essentially identical.

Comparing the curves in Fig. 11 with those from the temperature dependence study displayed in Fig. 10 reveals the parallel trends in the emission profile between increasing laser power and increasing temperature. The difference between the 44.7 mW and 0.3 mW spectra looks quite comparable but shifted slightly more to the difference between the 25 ºC and 22.5 ºC spectra. Based on this, the temperature of the glass artifact in the laser illumination volume is presumed to have stabilized approximately 2.5 ºC to 3 ºC above ambient temperature at this laser power.

An additional laser power study was conducted using the micro-scale configuration where the spot size ($1/e^2$ diameter) was not directly measured but was estimated to be approximately 5 µm at the focal plane based on the beam diameter and numerical aperture of the objective. Spectra were collected at a series of laser power levels in the same manner as in the macro-scale study. An example result from this study is displayed in Fig. 12.

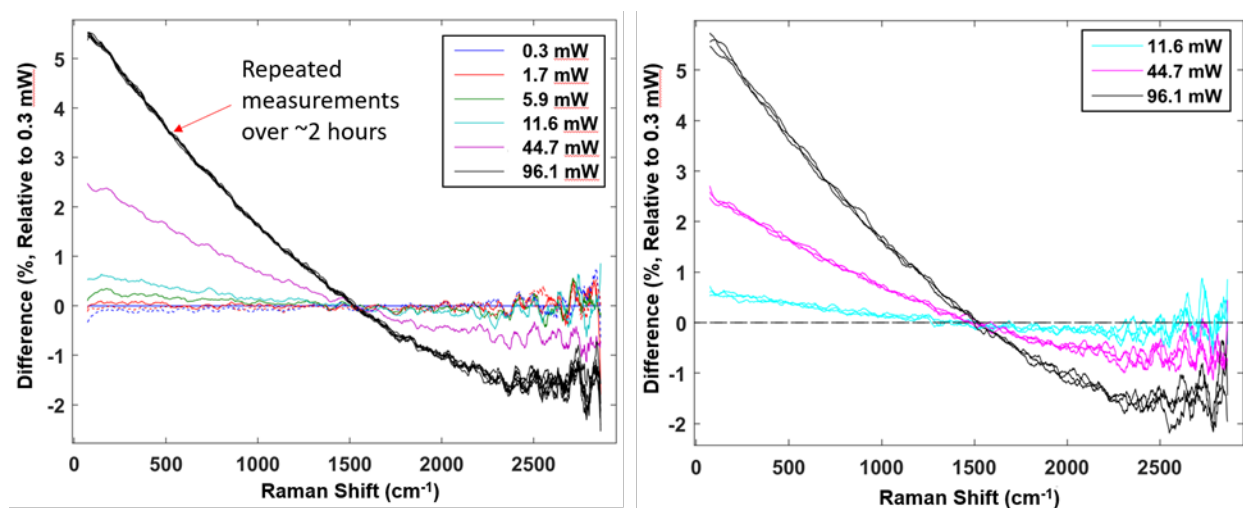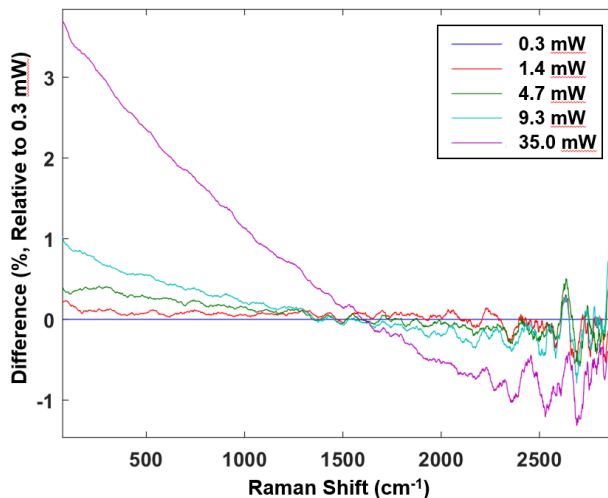**Fig. 12.** Spectral Shifts as a Function of Laser Power in the Micro-Scale configuration.

Difference spectra of one SRM 2246a unit when excited at different laser powers relative to measurements conducted at the lowest laser power. These data were collected on the alternate configuration of the instrument utilizing a 4X microscope objective.

The trends and presumed heating effects are very similar to those with the macro-scale configuration, but the effects are somewhat more significant at lower power levels. However, the differences between the two measurement configurations would be less than two-fold at the same total laser power. This result was somewhat surprising given that the laser power densities in this micro configuration are approximately 2500 times higher than the macro configuration. Prior investigations on a micro-Raman system led to an incorrect assumption that the potential impacts of higher laser powers would be significantly reduced in measurement scenarios where laser spot sizes were hundreds to thousands of micrometers. The results shown here, and similar observations reported from users of SRM 2246, suggest otherwise.

There may be a modellable relationship of temperature effects based on both laser power density and focal volume, but it would be difficult to make use of this in practice. It is currently not possible to give a specific recommendation for maximum laser power density. Users need to measure emission spectra at varying laser powers and look for peak shifts in the relative emission profile and then keep laser power levels below the point when perturbations become detectable or, alternatively, below a user specified tolerance.

Based on these investigations, maximum laser powers were set to minimize significant laser induced temperature effects. When collecting spectra for characterizing the emission spectrum, the laser power was limited to 5.9 mW in the macro-scale configuration and 1.4 mW in the micro-scale configuration. Potential impacts from laser induced heating were not explicitly included when establishing the uncertainties.

For the homogeneity assessment on the XY-stage configuration, a laser power of 4.7 mW was used to avoid excessive data acquisition times.

An important note about potential laser heating effects is that the spectra were all response corrected relative to spectra collected from either multiple SRM 2246 units or a reference 2246a unit under the same conditions, laser power, and at the same time. Consequently, any laser induced temperature changes are expected to be consistent between the reference and test units. This serves to minimize any impact of the changes on the response-corrected spectra.

4.4. Corrected SRM 2246a Spectrum and Model Determination

The data used to characterize the corrected SRM 2246a luminescence spectrum and establish the certified model are summarized in Table 2.

Table 2. Summary of Spectra Used in Model Determination.

Set	Configuration	Raman Shift Ranges	# Units Used	
			2246a	2246
1	Macro-Scale	(68 to 2882) cm^{-1} (1527 to 3750) cm^{-1}	7	5
2	Macro-Scale	(68 to 2882) cm^{-1} (1309 to 3618) cm^{-1}	9	5
3	Micro-Scale	(60 to 2874) cm^{-1} (1309 to 3618) cm^{-1}	10	6

All data used for certifying the emission spectrum of SRM 2246a were response corrected using measured units of SRM 2246. Corrected spectra of SRM 2246 using a calibrated irradiance source were generated but used only for the purposes of confirming SRM 2246 stability.

A lognormal based model was used to model the corrected luminescence spectrum of SRM 2246 and was also utilized for SRM 2246a. The model was utilized in the certification of SRMs 2245 2242a, and 2246. The linearly-shifted lognormal model used to describe the mean shape of the luminescence spectrum of SRM 2246a when excited at 830 nm is:

$$I(\Delta\upsilon) = H \cdot e^{\left[\frac{-\ln 2}{(\ln\rho)^2}\left(\ln\left[\frac{(\Delta\upsilon - x_0)(\rho^2 - 1)}{w*\rho} + 1\right]\right)^2\right]} + m \cdot \Delta\upsilon + b \tag{1}$$

where $\Delta\upsilon$ is wavenumber in Raman shift, H is peak height, w is peak width, ρ is half-width ratio, x_0 is a location parameter for the lognormal distribution while m and b are the slope and intercept terms, respectively, for the linear term.

The estimated parameter values and the techniques used derive them are presented in Section 6. These values are considered to adequately describe the luminescence spectrum from (110 to 3000) cm^{-1} Raman shift relative to 830 nm in the temperature range of 20 ºC to 25 ºC. The model curve and the high and low extreme spectra for each of the three datasets used to define the model are displayed in Fig. 13.
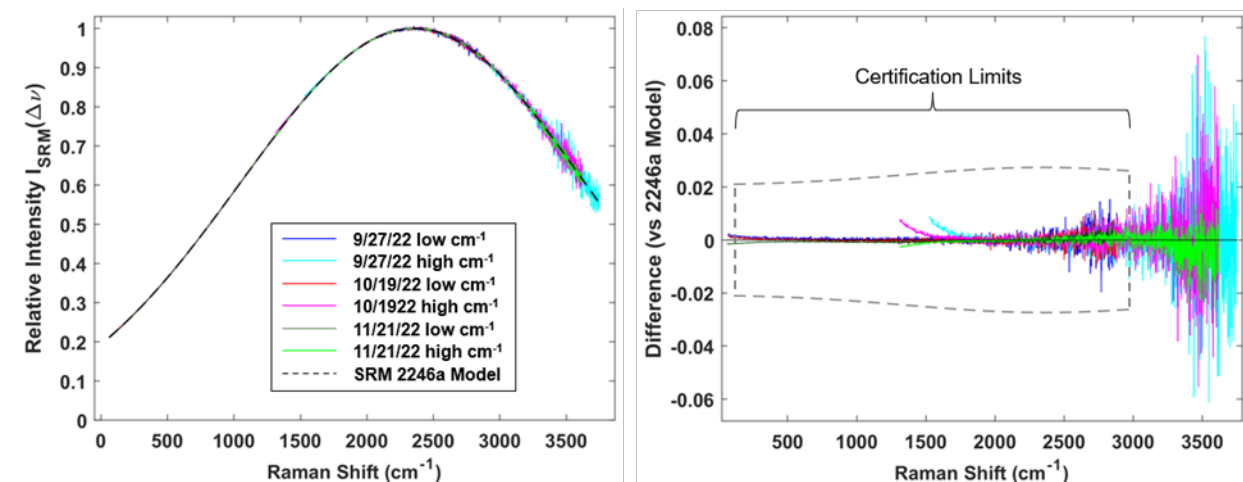
Fig. 13. Comparison of Observed Spectra with the Luminescence Model Curves.

Left Panel: The SRM 2246a lognormal model overlaid on the average corrected SRM 2246a spectrum from each of the certification datasets. Data was collected at two overlapping spectral regions each day.

Right Panel: The same data centered about the certified model. The 95% confidence bands (dashed gray lines) are included for comparison.

5. Uncertainties and Model Fitting

SRM 2246a is the first member of the 224x family to be certified relative to a previous member of the series. In addition, the certification is being conducted on a single instrument, although two distinct optical configurations were used. The emission models for all previous members of the SRM 224x series were defined using at least two and as many as four unique spectrometer systems. This required a considerable effort in terms of instrument setup, calibration, data collection and analysis. The use of multiple dissimilar spectrometer systems in the past, and the variation in the corrected spectra between them, was one of the primary sources of uncertainty in the certified emission model. The consensus statistical methods to estimate the uncertainties have also evolved over time, generally towards less conservative estimates; the resulting uncertainties may not have adequately covered the expected variability in emission profile.

Therefore an uncertainty budget has been developed explicitly for SRM 2246a. The budget consists of one "Type A" component (evaluated by application of statistical methods to experimental data, consistently with a measurement model [14]) and four "Type B" components (evaluated through elicitation of expert knowledge, authoritative sources including calibration certificates, certified reference materials, and technical publications and its distillation into probability distributions or fit-for-purpose summaries that describe states of knowledge about the true values of the inputs [14]).

The estimation of the Type A component is described in Section 6.2.3.

5.1. Type B Uncertainties

With the exception of the calibration source, the Type B components were estimated as constants across the spectrum in relation to the mean corrected or model normalized to have a maximum intensity of unity. The calibration source uncertainty component was derived from the source calibration data report and is relative to the intensity of the corrected emission spectrum (or model).

5.1.1. Homogeneity

The uncertainty associated with between-unit homogeneity was estimated from the observed between-unit variability across all 113 accepted units (see Section 3.1). Approximately 95 % of the difference spectra, $I_{unit}(\Delta v) - I_{SRM}(\Delta v)$, are completely within ±0.003 throughout the (110 to 3000) cm^{-1} range. This "expanded uncertainty" (U_{95}) is divided by 2 to assign the standard uncertainty (u) of the homogeneity component as 0.0015. This analysis is depicted in Fig. 14.
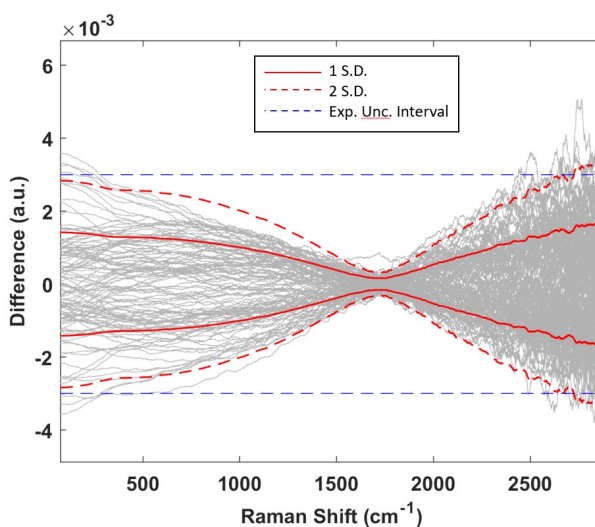
Fig. 14. Homogeneity-Related Uncertainty Component.
The light gray curves represent the difference spectra of the 113 accepted SRM 2446a units. The horizontal dashed lines bound the estimated U_{95} expanded uncertainty interval. The solid "hour glass" lines represent ±1 standard deviation across the difference spectra; the dashed curves represent ±2 standard deviations.

5.1.2. Temperature Dependence

The uncertainty associated with temperature dependence within the range (20 to 25) °C was estimated from the observed average differences observed at 20 °C and 25 °C (see Section 3.2). Approximately 95 % of the difference spectra, $I_{unit}(\Delta v) - I_{SRM}(\Delta v)$, at these endpoint temperatures are completely within ±0.006 throughout the (110 to 3000) cm^{-1} range. This "expanded uncertainty" (U_{95}) is divided by 2 to assign the standard uncertainty (u) of the homogeneity component as 0.003. This analysis is depicted in Fig. 15.

Fig. 15. Temperature Dependence-Related Uncertainty Component.

The solid curves represent the average difference spectra of three SRM 2446a units at (20.0, 22.5, and 25.0) °C. The light dotted lines represent the difference spectra of the individual units. The horizontal dashed lines bound the estimated U_{95} expanded uncertainty interval.

5.1.3. Linearity/Geometry

The uncertainty associated with Raman spectrometer linearity and/or geometry differences is estimated from the differences among three spectrometer systems utilized in the certification of SRM 2246. These systems included both commercial and purpose-built spectrometer systems comprising varying optical configurations, spectrographs, and detectors with illumination/collection volumes spanning the micron to millimeter scales. The sources of the differences observed between these instruments are not known but likely include effects such as positioning sensitivity of the SRM units and calibration source, detector non-linearity, differences in matching the geometry between the collected SRM emission and the emission from the calibrated light source, and temperature gradients.

Approximately 95 % of the average difference spectra, $I_{\text{instrument}}(\Delta v) - I_{\text{SRM}}(\Delta v)$, for these instruments are within ±0.015 throughout the (110 to 3000) cm^{-1} range. This "expanded uncertainty" (U_{95}) is divided by 2 to assign the standard uncertainty (u) of the homogeneity component as 0.0075. This analysis is depicted in Fig. 16.
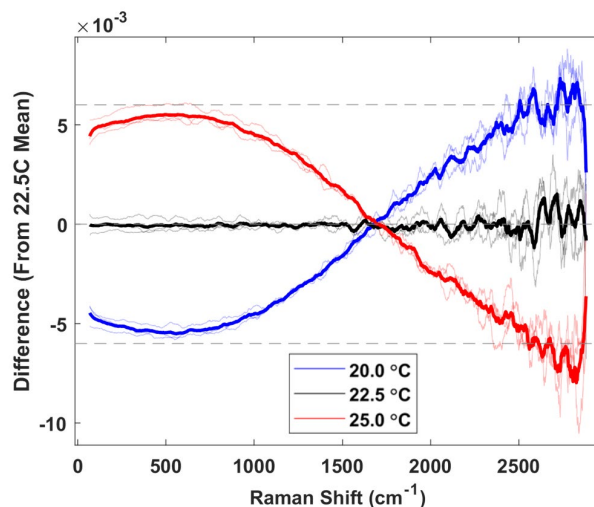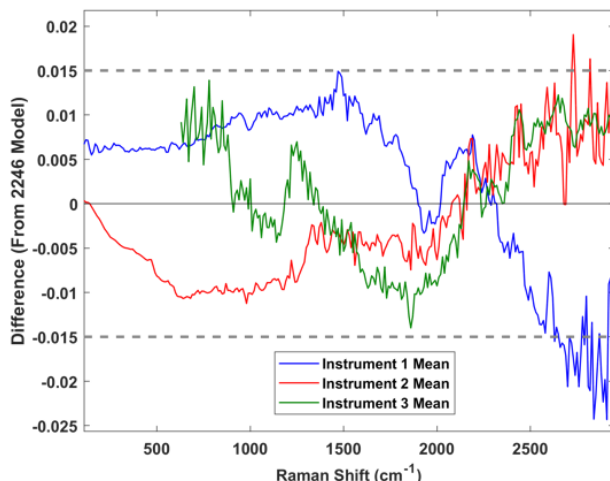
Fig. 16. Inter-instrument Variability-Related Uncertainty Component.

The solid curves represent the average difference spectra of three instruments used to certify the SRM 2246 model. The horizontal dashed lines bound an estimated ±95 % expanded uncertainty interval.

5.1.4. Calibrated Light Source

An uncertainty component was estimated based on the NIST-calibrated light source used in the certification of SRM 2246 and all previous SRMs in this series. The source is calibrated for spectral irradiance over the range of 300 nm to 2000 nm at 5 nm spacing with data provided in units of $\mu W \cdot cm^{-2} \cdot nm^{-1}$ and provides metrological traceability to the NIST spectral irradiance scale [15]. The relative uncertainty of the calibration varies smoothly with wavelength across the range. Table 3 lists the values within the approximately (830 to 1105) nm spectral region of interest for certification. The maximum value of the relative standard uncertainty (u_{rel}) within this region, 0.725 %, is used as calibration source uncertainty across the spectral range. The associated approximate 95 % confidence expanded relative uncertainty (U_{95rel}) is estimated as twice u_{rel}.

Table 3. Irradiance Data for the Calibrated Light Source.

Wavelength (nm)	Raman Shift (cm^{-1})	Irradiance ($\mu W\ cm^{-2}\ nm^{-1}$)	u_{rel}	U_{95rel}
830	0	0.1513	0.570 %	1.14 %
900	937	0.1613	0.540 %	1.08 %
950	1522	0.1667	0.635 %	1.27 %
1000	2048	0.1697	0.725 %	1.45 %
1050	2524	0.1705	0.720 %	1.44 %
1105	2998	0.1689	0.710 %	1.42 %

6. Statistical Analysis

This report provides a summary of the analysis used to determine the certifiable spectrum for SRM 2246a and the associated uncertainty. The uncertainly analysis incorporates contributions from both statistical (Type A) and calibration (Type B) sources. Section 6.1 provides a summary of the results of the statistical data analysis and uncertainty assessment. In Section 6.2 we describe the data the model was derived from, the methods employed for the Type A evaluation, and the uncertainty components evaluated by Type B methods. After combining these uncertainty components in root of sum squares, the results are expressed as a confidence band.

6.1. Estimates

6.1.1. Coefficient Values

The values of the coefficients of the linearly shifted lognormal model describing the mean shape of the luminescence spectrum of SRM 2246a, excited at 830 nm, are listed in Table 4. The spectrum and its associated 95% expanded uncertainty bands are shown in Fig. 17. The mean half-width of the confidence band amounts to 8% of the mean shape. The dependent variable in this model is the relative spectral intensity of the luminescence. The independent variable is the wavenumber expressed in units of Raman shift (cm^{-1}) from the laser excitation wavelength 830 nm. This model will be certified to describe the luminescent response of SRM 2246a between (110 and 3000) cm^{-1} Raman shift at temperatures of (20 to 25) °C.[1]

Table 4. Coefficients of the Linearly Shifted Lognormal Certified Model.

Parameter	95 % Lower Band	Mean Shape	95 %Upper Band
H	1.0142	1.0178	1.0213
w	3091.9	3082.3	3072.9
ρ	0.98303	0.98252	0.98201
x_0	2353.7	2353.1	2352.6
m	-0.00000043629	-0.00000011825	0.00000020664
b	-0.035124	-0.017500	0.000093692

---

1 This model includes values for the *m* and *b* parameters of Eq 1 that are not statistically significantly different from zero as exemplified by their confidence interval including zero. However, this does not imply that they are equal to zero and have no associated uncertainty. To stay consistent with previous members of the SRM 224x family (and with this inclusion of uncertainty in mind), these linear shift parameters are included in the model. The inclusion of these parameters did not negatively affect the model fit.
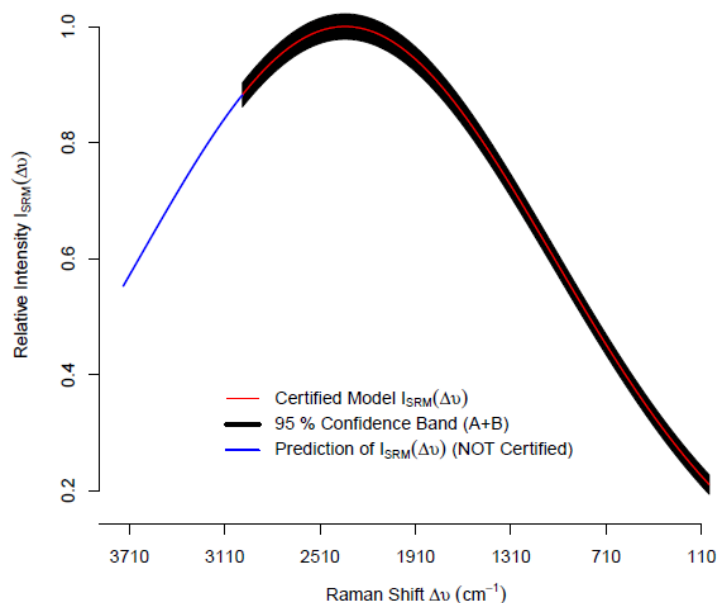
Fig. 17. Certified Model Describing the Luminescence Spectrum of SRM 2246a.

The Raman shift is shown on the X-axis (cm^{-1}) and the relative intensity is shown on the Y-axis. The red line in the center corresponds to the proposed linearly-shifted lognormal model, and the solid black band immediately around it the 95% confidence interval. The confidence interval incorporates information about both Type A and B uncertainties. The solid blue line corresponds to the predicted behavior beyond the model's (110 and 3000) cm^{-1} interval of validity.

6.1.2. Uncertainty

The combined standard measurement uncertainty comprises one component evaluated by application of Type A (statistical) methods, and one component evaluated by Type B (other) methods, combined in root sum of squares. The former subsumes contributions attributable to differences between the dates of measurement and variations in instrument configuration used in the certification process, and contributions from uncontrolled factors, all of which find expression in the dispersion of values of luminescent intensity that were obtained experimentally. The latter includes contributions from several sources discussed in Section 5.1; their values are summarized Table 5.[2] Except for the Calibration Source, components were estimated as uniform, symmetric intervals around the corrected SRM spectrum with a peak maximum of 1.

Table 5. Type B Uncertainty Budget from Various Sources.

Source	Type	Standard Uncertainty	DF
Homogeneity	Absolute	0.0015	∞
Temperature	Absolute	0.0030	∞
Linearity/Geometry	Absolute	0.0075	∞
Calibration Source	Relative	0.725%	∞

---

2 In all previous SRM 224x family model evaluations, the only Type B component considered was the uncertainty in the white-light, uniform-source, integrating sphere irradiance calibration (noted in Table 5 as Calibration Source), assessed at 1.1% expanded uncertainty of the certified value.

The model was obtained by fitting the function defined by Eq. 1 to measured values of $I_{2246a}(\Delta v)$ made on three different days but on the same instrument. The fitting method was (unweighted) nonlinear least squares. The associated uncertainty expresses components for which some were evaluated by Type A methods and other by Type B methods, combined in accordance with reference [16]. The Type A evaluations were performed using a Monte Carlo method consistent with reference [17], and by application of standard methods for uncertainty analysis for linear and nonlinear statistical models [18].

6.2. Analysis

6.2.1. Data

As described in Section 4.4, the data used to define the model consists of measurements of relative intensity made at each value of the Raman shift Δv on three separate dates. Altogether, there are 8,019 measured values: 2678 each from Sets 1 and 2, 2663 from Set 3. Each of these measured values is an average of repeated instrumental readings. However, since it is questionable whether they represent statistically independent replicates, neither the number of such repeats, nor the corresponding standard deviations, are used in this study.

In total, 10 units of SRM 2246a and 6 units of SRM 2246 were utilized in the certification measurements for the SRM 2246a corrected emission spectrum. Specifically, 7 units of SRM 2246a and 5 units of SRM 2246 were measured in Set 1. In Set 2, 3 additional units of SRM 2246a were added to the measurement set but the data for 1 of these units was not usable. For Set 3, an additional unit of SRM 2246 was included and a total of 10 units of SRM 2246a and 6 units of SRM 2246 were measured (Table 3). The measurements from Sets 1 and 2 correspond to data collected with identical instrument configurations (the "macro" configuration), although the longer wavelength grating position is different between the two. The data in Set 3 used a different optical setup (the "micro" configuration) that sampled a significantly smaller area than that used for Sets 1 and 2. In this setup, spectra were not collected from a single central location but instead were collected from 32 distinct points in a grid around the center of the unit. At each location, two repeat spectra were collected.

6.2.2. Model

The model used to describe the mean shape is of the form given in Eq. 1. If, $x_1, \ldots, x_m$ denote the Raman shift Δv relative to 830 nm excitation at which the measured values of $I_{2246a}(\Delta v)$ were $y_1, \ldots, y_m$, then the statistical model is

$$y_i = f(x_i, H, w, \rho, x_0, m, b) + \epsilon_i \tag{2}$$

where f is the function defined on the right-hand side of Eq. 1 and $\epsilon_1, \ldots, \epsilon_m$ denote measurement errors assumed to be realized, albeit non-observable, values of independent Gaussian random variables all with mean zero and unknown variance, assumed constant across the scale of Raman shifts.

This nonlinear regression model was fitted by unweighted least squares, using function nls from the R environment for statistical computing and graphics [19], employing a Gauss-Newton algorithm. The same model was also fitted using the Levenberg-Marquardt algorithm [20] as

implemented in the function nls.lm defined in the R package minpack.lm [21]. The two alternatives produced identical results up to five significant digits.

6.2.3. Type A Uncertainty Assessment

Once the statistical model defined in Eq. 2 is used to combine all the measurement results by means of a nonlinear regression, several conventional methods for uncertainty analysis immediately become available. Before describing the conventional methods used for the uncertainty analysis in this study, a few words of explanation regarding confidence and prediction bands may be in order.[3] Before the implementation of the various sources of Type B uncertainty in Table 5, only the calibration source was considered as a source of Type B uncertainty in the SRM 224x series and both the confidence and prediction bands were given. With the inclusion of the additional Type B uncertainty sources, a prediction band was deemed unnecessary.[4]

Just as the averaging of $n \geq 2$ independent measured values has a smaller associated uncertainty than a single measured value (typically $\sqrt{n}$ times smaller), the uncertainty associated with an estimated regression curve at any particular point will be smaller than the uncertainty of a single data point since the regression is a form of averaging.

A distinction that should be kept in mind is between a confidence interval for $I_{2246a}(\Delta v)$ at a particular value of Δv, and a simultaneous confidence band for the whole spectrum. The former may be relevant if one is interested in a specific, particularly sharp feature in the spectrum (say, to detect the presence of a certain compound based on a particular line), while the latter will be relevant when the whole spectrum is the object of interest. Typically, the width of a confidence interval built at a particular value of the Raman shift will be smaller than the width of the corresponding band built to simultaneously cover the whole spectrum.

The bands depicted in Fig. 17 and described in Table 4 cater to the case where the object of interest is the whole spectrum, and express all the recognized components of uncertainty, evaluated by either Type A or Type B methods.

6.2.4. Bootstrap

The first method used for uncertainty analysis was the statistical bootstrap [22,23], and involved sampling pairs $\{\Delta v, I_{2246a}(\Delta v)\}$ from the 8019 such pairs in the data, uniformly at random with replacement, to obtain a sample of the same size as the data, to which the Eq.1 model was fitted.

This process was repeated 100000 times, which produced 100000 sets of the estimated parameters (H, w, ρ, x_0, m, b), hence these many replicates of the fitted spectral shape. The 95 % confidence band was derived from this collection by creating the corresponding probability

---

3 Confidence bands originally produced by analyses of the SRM 224x series were obtained from confidence intervals built for $I_{2245a}(\Delta v)$ at each value of Δv, whose upper and lower endpoints were then smoothly joined by another member of the family of curves defined by Eq. 1. This uncertainty analysis does not account for the mean luminescence intensity varying smoothly according: the conventional confidence bands that typically are derived for straight regression lines use a different recipe altogether and the same holds for nonlinear regressions.

4 Prediction bands characterize the uncertainty of a single measurement of the spectrum (or spectrum as a whole) that may be made using methods and instruments generally comparable to those used in the certification process. With the inclusion of additional Type B components, this estimation was no longer deemed necessary.

envelopes as described in [22] and using the implementation readily available in the boot package [24].

6.2.5. Linearization

The second method that was used to compute the confidence bands (and in previous SRMs in this series, prediction bands) is based on local linearization of the nonlinear regression model [25] and implemented in the package nls2 [26]. After the bootstrap samples were found as described in the previous section, the local linearization of nls2 was used in order to find the upper and lower 95 % confidence bound parameter values listed in Table 4.

In the analysis of previous SRMs in this series, other methods of linearization of the nonlinear regression model were implemented for exploratory reasons. All of the methods performed comparably well, and so only the local linearization implemented in the nls2 package has been utilized.

6.2.6. Approximation

Similarly, for what happens for linear models [27, Figure 1.8], the functional form of the boundaries of confidence bands is different from the functional form of the regression function. In this case, and merely for reasons of convenience to the users of the certificate, these boundaries were approximated using Eq. 1, leading to the results in Table 4. As for the previous SRMs in the series, users may find the uncertainty bounds using the upper and lower 95% confidence values for the model parameters, and there is no separate table giving the interval for each value of the Raman shift.

6.2.7. Parameter Interdependence

The parameters of this model are not independent of one another. From the bootstrap replicates, variance/covariance, correlations, and marginal densities between each of the pairs of parameters can be found. The variance-covariance matrix given in Table 6. The distributions and correlation values are displayed in Fig. 18.

Table 6. Variance/Covariance Matrix of the Certified Parameter Values.

	H	w	ρ	x_0	m	b
H	4.5282E−05					
w	8.2959E−02	1.5326E+02				
ρ	3.3627E−05	6.1286E−02	3.3400E−05			
x_0	3.3224E−02	6.0390E+01	2.8261E−02	2.6322E+01		
m	-1.9698E-08	-3.5815E-05	-1.7380E-08	-1.5778E-05	9.5318E-12	
b	6.1861E-07	4.0261E-04	6.9275E-06	3.5842E-03	-2.5403E-09	5.3756E-06

The diagonal values are the variance components of each parameter while the off-diagonal values are the covariance components between each pair of model parameters. These values can be used in a multivariate Gaussian distribution by using the certified values as the mean and these values as the variance-covariance matrix.

Due to this interdependence, uniformly sampling between the upper and lower confidence bounds for each parameter will **not** always generate a curve that lies between the lower and

upper 95 % confidence bounds. To fit a continuous luminescence curve through discrete instrumental data using the Eq. 1 model, sample from multivariate Gaussian distributions using the certified values as the means and the values in Table 6 as the variance-covariance matrix.
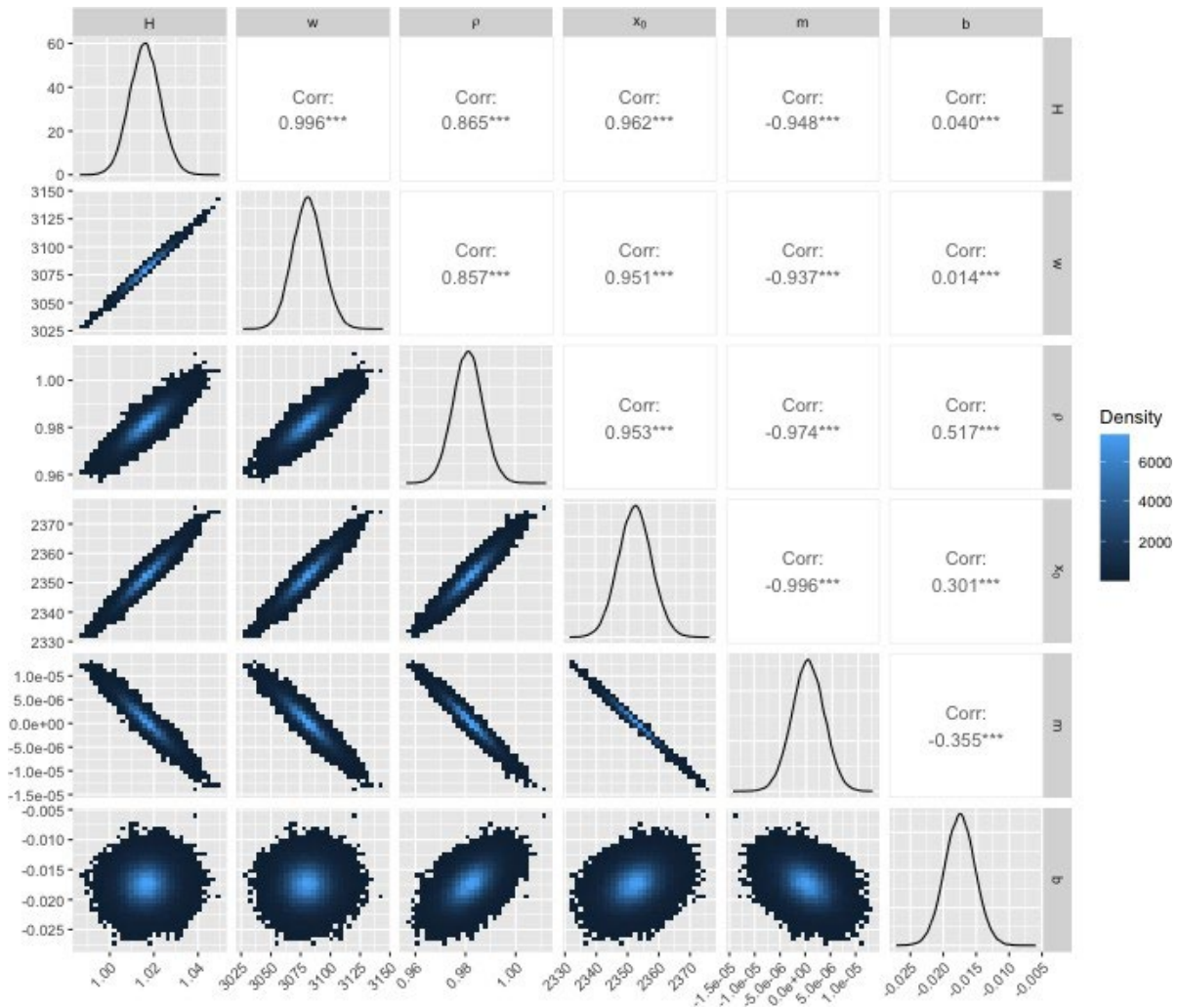
Fig. 18. Interdependence of the Model Parameters.

The lower portion of the matrix displays the marginal densities of each pair of parameter values (found from the 100 000 bootstrap replicates). The lighter blue color denotes higher density while the darker blue denotes lower density. The upper portion of the matrix displays their correlation values, with the three stars denoting statistical significance. The diagonal values are the densities of each of the parameters themselves.

7. Correction Functions

SRM 2246 is used to provide Raman spectra corrected for relative intensity. This requires a measurement of the filter's luminescence spectrum on the Raman instrument and then a mathematical treatment of both this observed luminescence spectrum and the observed Raman spectrum of the sample.

7.1. Calculation

The relative intensity of the measured Raman spectrum of the sample can be corrected for the instrument-specific response by a computational procedure that uses a correction curve. This curve is generated using the certified model and the measured luminescence spectrum of the SRM glass. For the spectral range of certification, $\Delta \upsilon = 110$ cm^{-1} to 3000 cm^{-1}, compute the elements of the certified relative mean spectral intensity of SRM 2246a, $I_{\text{SRM}}(\Delta \upsilon)$, according to Eq. 1 and the "Mean Shape" parameter values listed in Table **4**.

The elements of $I_{\text{SRM}}(\Delta \upsilon)$ are obtained by evaluating Equation 1 at the same data point spacing used for the acquisition of the luminescence spectrum of the SRM and of the Raman spectrum of the sample. The elements of the correction curve $I_{\text{CORR}}(\Delta \upsilon)$, defined by Equation 2, are obtained from $I_{SRM}(\Delta \upsilon)$ and the elements of the glass luminescence spectrum, $S_{\text{SRM}}(\Delta \upsilon)$, by

$$I_{\text{CORR}}(\Delta \upsilon) = I_{\text{SRM}}(\Delta \upsilon)/S_{\text{SRM}}(\Delta \upsilon) \ . \tag{3}$$

The elements of the intensity-corrected Raman spectrum, $S_{\text{CORR}}(\Delta \upsilon)$, are derived by multiplication of the elements of the measured Raman spectrum of the sample, $S_{\text{MEAS}}(\Delta \upsilon)$, by the elements of the correction curve [28]

$$S_{\text{CORR}}(\Delta \upsilon) = S_{\text{MEAS}}(\Delta \upsilon) \cdot I_{\text{CORR}}(\Delta \upsilon) \ . \tag{4}$$

7.2. Uncertainty Propagation

Approximate 95 % level of confidence expanded uncertainty bounds for the corrected Raman spectrum, $S_{\text{CORR}}(\Delta \upsilon)$, can be estimated using the procedure describe above, but using the "95 % Lower Bound" and then the "95 % Upper Bound" parameter values listed in Table **4** instead of the "Mean Shape" values.

References

[1] National Institute of Standards and Technology (7 January 2022) Certificate of Analysis, Standard Reference Material® 2241 Relative Intensity Correction Standard for Raman Spectroscopy: 785 nm Excitation. https://tsapps.nist.gov/srmext/certificates/2241.pdf.

[2] National Institute of Standards and Technology (22 October 2013) Certificate of Analysis, Standard Reference Material® 2242 Relative Intensity Correction Standard for Raman Spectroscopy: 532 nm Excitation. https://tsapps.nist.gov/srmext/certificates/archives/2242.pdf.

[3] National Institute of Standards and Technology (15 October 2019) Certificate of Analysis, Standard Reference Material® 2242a Relative Intensity Correction Standard for Raman Spectroscopy: 532 nm Excitation. https://tsapps.nist.gov/srmext/certificates/2242a.pdf.

[4] National Institute of Standards and Technology (11 June 2009) Certificate of Analysis, Standard Reference Material® 2243 Relative Intensity Correction Standard for Raman Spectroscopy: 488 nm and 514.5 nm Excitation. https://tsapps.nist.gov/srmext/certificates/archives/2243.pdf.

[5] National Institute of Standards and Technology (20 August 2020) Certificate of Analysis, Standard Reference Material® 2244 Relative Intensity Correction Standard for Raman Spectroscopy: 1064 nm Excitation. https://tsapps.nist.gov/srmext/certificates/2244.pdf.

[6] National Institute of Standards and Technology (23 August 2016) Certificate of Analysis, Standard Reference Material® 2245 Relative Intensity Correction Standard for Raman Spectroscopy: 633 nm Excitation. https://tsapps.nist.gov/srmext/certificates/archives/2245.pdf.

[7] National Institute of Standards and Technology (14 September 2020) Certificate of Analysis, Standard Reference Material® 2246 Relative Intensity Correction Standard for Raman Spectroscopy: 830 nm Excitation. https://tsapps.nist.gov/srmext/certificates/2246.pdf.

[8] ASTM E2911-23 Standard guide for relative intensity correction of Raman spectrometers. ASTM International: West Conshohocken, PA. https://doi.org/10.1520/E2911-23

[9] Yoon H, Gibson C (2011), SP250 Spectral Irradiance Calibrations, Special Publication (NIST SP), National Institute of Standards and Technology, Gaithersburg, MD, [online], https://doi.org/10.6028/NIST.SP.250-89

[10] Choquette SJ, Etz ES, Hurst WS, Blackburn DH, Leigh SD (2007) Relative Intensity Correction of Raman Spectrometers: NIST SRMs 2241 Through 2243 for 785 nm, 532 nm, and 488 nm/514.5 nm Excitation. Appl Spec 61(2): 117-129. https://doi.org/10.1366/000370207779947585

[11] Sansonetti CJ, Salit ML, Reader J (1996) Wavelengths of spectral lines in mercury pencil lamps. Appl Opt 35(1):74-77. https://doi.org/10.1364/AO.35.000074.

[12] Saloman EB, Sansonetti CJ (2004) Wavelengths, energy level classifications, and energy levels for the spectrum of neutral neon. J Phys Chem Ref 33(4):1113-1158. https://doi.org/10.1063/1.1797771.

[13] ASTM E1840-96 (2014) Standard Guide for Raman Shift Standards for Spectrometer Calibration. ASTM International: West Conshohocken, PA. https://doi.org/10.1520/E1840-96.

[14] Possolo A (2015) Simple Guide for Evaluating and Expressing the Uncertainty of NIST Measurement Results. (National Institute of Standards and Technology, Gaithersburg, MD), NIST Technical Note (NIST.TN) 1900. https://doi.org/10.6028/NIST.TN.1900.

[15] Report of Calibration, 39060S Special Tests of Radiometric Sources for Labsphere Model US-060-SL, Serial #LS1, NIST Test No: 685/288702-16. National Institute of Standards and Technology, Gaithersburg, MD.

[16] JCGM 100:2008 (2008) Evaluation of measurement data — Guide to the expression of uncertainty in measurement. Joint Committee for Guides in Metrology. https://www.bipm.org/en/publications/guides.

[17] JCGM 101:2008 (2018) Evaluation of Measurement Data — Supplement 1 to the "Guide to the Expression of Uncertainty in Measurement" – Propagation of distributions using a Monte Carlo method, Joint Committee for Guides in Metrology (JCGM). https://www.bipm.org/en/publications/guides.

[18] Venables WN, Ripley BD. (2002) Modern Applied Statistics with S, fourth ed. Springer, New York. ISBN 0-387-95457-0. https://doi.org/10.1007/978-0-387-21706-2.

[19] R Core Team (2023). R: A language and environment for statistical computing. R Foundation for Statistical Computing, Vienna, Austria. Available online at https://www.R-project.org/.

[20] Moré JJ (1978) The Levenberg-Marquardt algorithm: Implementation and theory. In: Watson GA (eds) Numerical Analysis. Lecture Notes in Mathematics, vol 630. Springer, Berlin, Heidelberg, pp. 105–116. https://doi.org/10.1007/BFb0067700.

[21] Elzhov TV, Mullen KM, Spiess A-N, Bolker B (2022) minpack.lm: R Interface to the Levenberg-Marquardt Nonlinear Least-Squares Algorithm Found in MINPACK, Plus Support for Bounds, R package version 1.2-2. https://cran.r-project.org/web/packages/minpack.lm/minpack.lm.pdf.

[22] Davison AC, Hinkley DV (1997) Boostrap methods and their applications. Cambridge University Press, New York. https://doi.org/10.1017/CBO9780511802843.

[23] Efron B, Tibshirani RJ (1993) An Introduction to the Bootstrap. No. 57 in Monographs on Statistics and Applied Probability. Chapman & Hall/CRC, Boca Raton, Florida. https://doi.org/10.1201/9780429246593.

[24] Canty A, Ripley BD (2022) boot: Bootstrap R (S-Plus) Functions, R package version 1.3-28.1. https://cran.r-project.org/package=boot.

[25] Bates D, Watts D (1988) Nonlinear Regression Analysis and its Applications. Wiley Series in Probability and Mathematical Statistics. John Wiley & Sons, New York, NY. https://doi.org/10.1002/9780470316757.

[26] Grothendieck G (2022) nls2: Non-Linear Regression with Brute Force. R package version 0.3-3. https://cran.r-project.org/web/packages/nls2/nls2.pdf.

[27] Draper N, Smith H (1998) Applied Regression Analysis, 3rd ed. A Wiley-Interscience publication. Wiley, New York. https://doi.org/10.1002/9781118625590.

[28] Frost KJ, McCreery RL (1998) Calibration of Raman Spectrometer Response Function with Luminescence Standards: An Update. Appl Spectrosc 52:1614–1618. https://doi.org/10.1366/0003702981943121.

Appendix A. List of Symbols, Abbreviations, and Acronyms

$\Delta\upsilon$	wavenumber in Raman shift
ϵ_i	i^{th} measurement error
ρ	half-width ratio
b	intercept
f	function (Eq. 1)
H	peak height
$I_{\text{x}}(\Delta\upsilon)$	emission intensity at $\Delta\upsilon$ for Raman spectrum of type "x"
m	slope
$S_{\text{x}}(\Delta\upsilon)$	Raman spectrum of type "x" at $\Delta\upsilon$
u	standard uncertainty
u_{rel}	relative standard uncertainty, expressed as a percentage
U_{95}	approximate 95 % confidence expanded uncertainty
$U_{95\text{rel}}$	approximate 95 % confidence relative expanded uncertainty
w	peak width
x_0	location parameter for the lognormal distribution
x_i	i^{th} independent variable
y_i	i^{th} dependent variable
CCD	charge-coupled device
NIST	National Institute of Standards and Technology
PTFE	polytetrafluoroethylene
SRM	Standard Reference Material